

Chenchen Liu<sup>1</sup>  
Yoshinori Yamaguchi<sup>2,3</sup>  
Xifang Zhu<sup>4</sup>  
Zhenqing Li<sup>1</sup>  
Yi Ni<sup>2</sup>  
Xiaoming Dou<sup>2,4\*</sup>

<sup>1</sup>Engineering Research Center of Optical Instrument and System, University of Shanghai for Science and Technology, Shanghai, P. R. China

<sup>2</sup>Institute of Photonics and Biomedicine (IPBM), Graduate School of Science, East China University of Science and Technology (ECUST), Shanghai, P. R. China

<sup>3</sup>Department of Applied Physics, Graduate School of Engineering, Osaka University, Yamadaoka, Suita-city, Osaka, Japan

<sup>4</sup>School of Optoelectronic Engineering, Changzhou Institute of Technology, Changzhou, Jiangsu, P. R. China

Received November 18, 2014

Revised March 18, 2015

Accepted March 18, 2015

## Research Article

# Analysis of small interfering RNA by capillary electrophoresis in hydroxyethylcellulose solutions

The analysis of small interfering RNA (siRNA) is important for gene function studies and drug developments. We employed CE to study the separation of siRNA ladder marker, which were ten double-stranded RNA (dsRNA) fragments ranged from 20 to 1000 bp, in solutions of hydroxyethylcellulose (HEC) polymer with different concentrations and molecular weights (*M<sub>w</sub>*). Migration mechanism of dsRNA during CE was studied by the mobility and resolution length (*RL*) plots. We found that the *RL* depended on not only the concentration of HEC, but also the *M<sub>w</sub>* of HEC. For instance, *RL* of small dsRNA fragment was more influenced by concentration of high *M<sub>w</sub>* HEC than large dsRNA fragment and *RL* of large dsRNA fragment was more influenced by concentration of low *M<sub>w</sub>* HEC than small dsRNA fragment. In addition, we found electrophoretic evidence that the structure of dsRNA was more compact than dsDNA with the same length. In practice, we succeeded to separate the glyceraldehyde 3-phosphate dehydrogenase siRNA in the mixture of the siRNA ladder marker within 4 min.

### Keywords:

Capillary electrophoresis / double-stranded RNA / double-stranded DNA / Hydroxyethylcellulose / small interfering RNA DOI 10.1002/elps.201500018



Additional supporting information may be found in the online version of this article at the publisher's web-site

## 1 Introduction

Small interfering RNA (siRNA) is vastly investigated in gene function studies and drug developments because siRNA triggers RNA interference (RNAi). RNAi is a highly efficient gene silencing mechanism, in which RNA molecules inhibit gene expression resulting in the destruction of specific mRNA molecules [1]. In 1999, David Baulcombe and coworker discovered that short double-stranded RNA (dsRNA), which was named as siRNA, functioned in the pathway of RNAi by breaking down cognate mRNA molecules of target gene [2]. In 2001, Tuschl and coworkers reported that synthetic siRNA induced RNAi in mammalian cells [3]. In theory, any target gene can be knocked down by siRNA with a complementary sequence because RNAi mechanism is a highly specific gene

silence process. As a result, RNAi executed by introducing siRNA into mammalian cells has grown to a hot topic in the field of antiviral therapy, cancer treatment, and biopharmaceutics [1, 4, 5].

siRNA is classified as dsRNA that consists of a double strand region of 19 bp with 2 nt 3' overhangs at both ends [6]. Several methods have been employed for dsRNA identification, such as ELISA, slab gel electrophoresis [7], and molecular hybridization. While those methods have been used for dsRNA applications, CE is gradually recognized as a powerful method for nucleic acid analyzing by researchers because of its property of high efficiency, high throughput, and high sensitivity [8–13]. CE has been employed for studying dsDNA, ssDNA, and single-stranded RNA (ssRNA), and CE has been commercialized for DNA sequencing, SSCP, and RFLP analysis [14–16]. CE also has a great potential of integration for microchip device [17–19] that entitles itself a promising candidate for dsRNA analysis and RNAi research.

Because dsRNA and dsDNA possess the similar duplex structure formed by two nucleotide strands coiling around each other, it has been theoretically explained that their

**Correspondence:** Dr. Yoshinori Yamaguchi, Department of Applied Physics, Graduate School of Engineering, Osaka University, Yamadaoka, Suita-city, Osaka 565-0871, Japan  
**E-mail:** yoshi.yamaguchi@ap.eng.osaka-u.ac.jp

**Abbreviations:** dsRNA, double-stranded RNA; GAPDH, glyceraldehyde 3-phosphate dehydrogenase; HEC, hydroxyethylcellulose; *M<sub>w</sub>*, molecular weight; *RL*, resolution length; siRNA, small interfering RNA; ssRNA, single-stranded RNA

\*Additional corresponding author: Dr. Xiaoming Dou  
E-mail: xiaomingdou@yeah.net

separation performance by CE is identical [20–22]. At the same time, there are evidences that structural differences between dsRNA and dsDNA can distinguish each other. For example, Vakonakis and LiWang reported that the hydrogen bonds of A:U base pairs of dsRNA were stronger than those of A:T base pairs of dsDNA [23]. As the secondary structure of nucleic acid is determined by the hydrogen bonds, dsRNA is packed more tightly than dsDNA at secondary structure. Besides, Nakano et al. demonstrated the melting temperature ( $T_m$ ), which reflected the stability of nucleic acid structure, of dsRNA was higher than the one of dsDNA with same sequence [24]. In fact, the structural tightness and stiffness of nucleic acids affect their migration behavior during CE as well. Thus, the comparison of the separation performance between dsRNA and dsDNA was required for understanding their mechanical properties in spatial confirmation.

The migration of dsDNA, ssDNA, and ssRNA in entangled polymer solutions has been studied [7, 21, 25–27]. In solution with a polymer concentration above the entanglement threshold, a dynamic network is formed as polymer chains entangled with each other. When the nucleic acid fragments migrate through the network, they interact with the polymer chains. Thus, the physical properties of the network, such as pore size and stiffness, dominate the migration behavior of nucleic acids. As for the separation of small nucleic acid fragments, polymer solutions with high concentration are required to provide a comparative pore size for nucleic acid molecular sieving. In addition to the polymer concentration, molecular weight ( $M_w$ ) of the polymer also differentiates physical properties of the network, such as stiffness and stability. Hydroxyethylcellulose (HEC) polymers are hydrophilic and preferable to produce high-concentrated aqueous solutions. In practice, the preparation of high-concentrated HEC polymer solutions is feasible because of its hydrophilic property, and the replacement of HEC capillary is advantageous against other polymers, such as polyacrylamide and poly(ethyleneoxide).

In this work, we demonstrated the separation of siRNA ladder marker, which contained ten dsRNA fragments ranged from 20 to 1000 bp, by CE in HEC solutions with different  $M_w$ s and different concentrations. Migration mobility and resolution length ( $RL$ ) for dsRNA were discussed by examining the influence of  $M_w$  and concentration of HEC as a sieving polymer for CE. We also compared separation performance between dsRNA and dsDNA. Furthermore, we applied CE to size analyzing of GAPDH (glyceraldehyde 3-phosphate dehydrogenase) siRNA sample in an adjusted CE condition.

## 2 Materials and methods

### 2.1 Reagent

Different  $M_w$ s of HEC (90, 250, 720, and 1300 k) were purchased from Sigma-Aldrich (St. Louis, MO, USA). Polymer solutions were prepared with a series of concentrations with  $0.5\times$  TBE (Bio-Rad, Hercules, USA) and stirred for at least

24 h before filling into capillary. The HEC solution contained  $2\times$  SYBR Green II (Invitrogen, Carlsbad, USA) at final concentration. Noncoding siRNA ladder marker and dsDNA sample contained ten dsRNA and 13 dsDNA fragments, respectively (Supporting Information 1), which were purchased from TAKARA (Dalian, China). We synthesized GAPDH siRNA from GenePhrama (Shanghai, China), which had a 19 bp dsRNA region and 2 nt 3' overhangs at both ends.

### 2.2 Instruments

Our home-built CE system was described in our previous papers [28–31]. Briefly, the CE system was based on the fluorescence microscope (DP73, Olympus, Tokyo, Japan). The light from mercury lamp on the microscope was filtered by an optical cube (U-MWIB3, Olympus) to transmit a wavelength of 460–495 nm for fluorescence excitation. The emission light from dye–nucleonic acid conjugate was collected by a  $100\times$  objective (MPlanFL N, Olympus) and detected by a PMT (H8249-101, Hamamatsu Photonics, Japan). The 75  $\mu\text{m}$  id fused silica capillary (Polymicro, Phoenix, AZ, USA) was prepared with a total length of 9 cm and an effective length of 6 cm. The inside of capillary was coated by polyacrylamide to eliminate EOF [32]. The capillary was flushed by ultrapure water before each run to avoid contamination. Raw data were automatically stored in the computer, and high voltage supplier for CE was operated by a LabVIEW software (National Instrument, Austin, TX, USA). The whole CE system was enclosed in a dark box at room temperature.

## 3 Results and discussion

The purpose for this work was to study the separation performance of dsRNA in HEC solutions and reveal the migration behavior of dsRNA during CE. Four  $M_w$ s of HEC polymer and different concentrations of HEC solution were employed in our experiment. Typical electropherograms of dsRNA (Fig. 1A to D) and dsDNA (Fig. 1E) migrating in HEC solutions were illustrated. Ten dsRNA fragments were fully separated in each  $M_w$  of HEC solution with high concentration. An unspecific peak was observed before the peak of 20 bp dsRNA fragment, which was inferred as impurities in the process of synthesizing or digesting sample.

We also observed that dsDNA migrated slower than dsRNA with the same fragment size (Fig. 1D and E). As we referred in the introduction, we noticed that the structure of dsRNA was more compact than dsDNA so that dsRNA molecules presented a more coiling configuration compared to dsDNA molecules with the same base pairs. When both dsRNA and dsDNA molecules collided with polymer chains, they entangled but the entanglement of dsRNA was more transitorily than dsDNA so that dsRNA migrated faster. By examining the  $RL$  difference between dsRNA and dsDNA, results indicated the separation of dsDNA obtained smaller

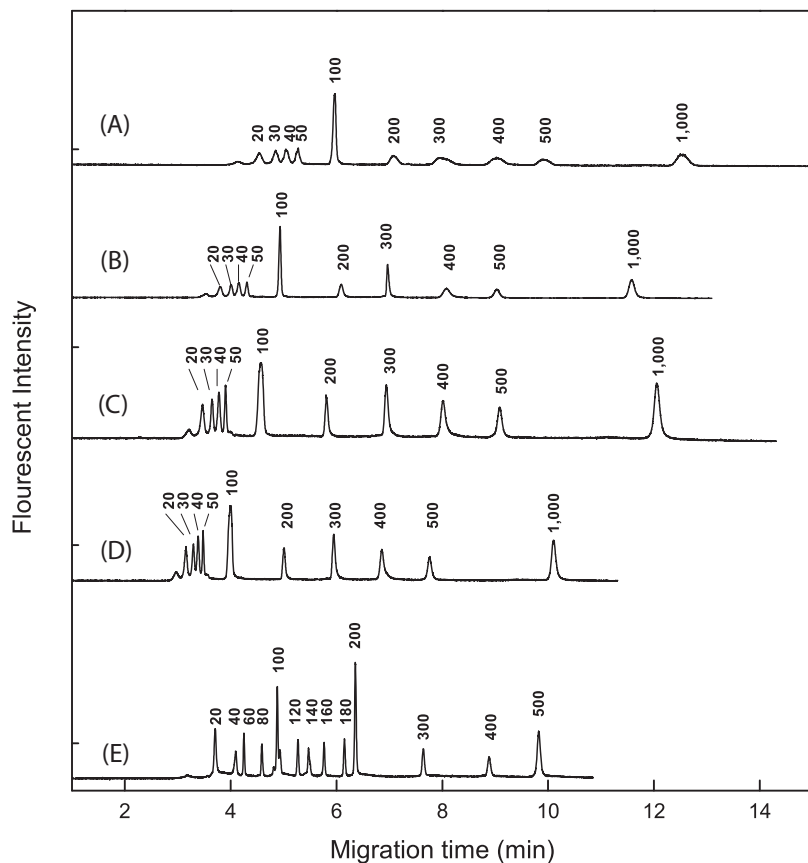


**Figure 1.** Capillary electropherogram of dsRNA fragments in HEC solution with (A) 4% concentration, 90 k *M<sub>w</sub>*, (B) 2% concentration, 250 k *M<sub>w</sub>*, (C) 1.4% concentration, 720 k *M<sub>w</sub>*, (D) 1.2% concentration, 1300 k *M<sub>w</sub>*, (E) capillary electropherogram of dsDNA fragments in 1300 k HEC solution with 1.2% concentration. In (A) and (B), the fluorescent intensity was, respectively, reduced to 1/2 and 1/3 of its original intensity. CE was performed at 100 V/cm. The total length and the effective length of the capillary were 9.0 and 6.0 cm, respectively. Sample was injected electrokinetically for 2.0 s at 100 V/cm.

RL than that of dsRNA (Supporting Information 2). Similar tendency was also observed in each *M<sub>w</sub>* of HEC solutions.

### 3.1 Mobility of dsRNA in HEC solutions

Mobility (Supporting Information 3) of dsRNAs identifies their migration regimes that dominate the separation performances during CE [33, 34]. Figure 2 illustrates mobility plot of dsRNA in 0.2–6% concentration and 90–1300 k *M<sub>w</sub>* of HEC solutions. In each *M<sub>w</sub>* of HEC solution two migration regimes were found. Those two regimes were corresponded to the Ogston regime (zone I) and reptation without orientation regime (zone II) [35–38], which were similar to that of dsDNA (Supporting Information 2).

As for polymer solutions with 250 k HEC, different concentrations ranged from 0.2 to 2.0% were tested to investigate the separation performance of dsRNA (Fig. 2B). According to the report from Todorov and Morris [25], the entanglement threshold of 250 k HEC polymer was among 0.08 and 0.3%. Therefore, in HEC solution between 0.2 and 0.4%, whose concentration was around the entanglement threshold, small dsRNA fragments (20–100 bp) were hardly resolved by CE separation. When the concentration of HEC polymer increased, a good separation performance was achieved as the slope of mobility plot was steeper. We found similar observation in solutions with other *M<sub>w</sub>*s of HEC.

The *M<sub>w</sub>* of HEC also dominated the mobility of dsRNA migration by observing the slope of mobility plots. The slope of the mobility curve reflected velocity difference between two adjoined peaks in the electropherogram. In all charts of Fig. 2, we observed that the slopes of small dsRNA (20–100 bp) fragments were more gentle as the *M<sub>w</sub>* of HEC increased, while the slopes derived from large dsRNA fragments (200–1000 bp) became steeper as the *M<sub>w</sub>* of HEC increased. This interpretation suggested that low *M<sub>w</sub>* HEC solutions were optimum to separate small dsRNA fragments, and high *M<sub>w</sub>* HEC solutions were optimum for separating large dsRNA fragments.

### 3.2 RL of dsRNA in HEC solutions

The analysis of RL [39] (Supporting Information 3) revealed the relationship between the separation capacity of CE and the HEC polymer with various *M<sub>w</sub>*s and concentrations. Here, RL between two adjacent peaks referred to the smallest resolvable size difference when  $R_s = 1$ , which was the “resolution per base.” From the plot of RL and dsRNA fragment size (Fig. 3), we found a tendency that RL ascended with the increase of dsRNA fragment size. In this work, the best RL for the whole range of dsRNA sample was achieved at 1.6% HEC (1300 k) polymer solution, which was from 3.0 bp (between 20 and 30 bp) to 17.1 bp (between 500 and 1000 bp). In our

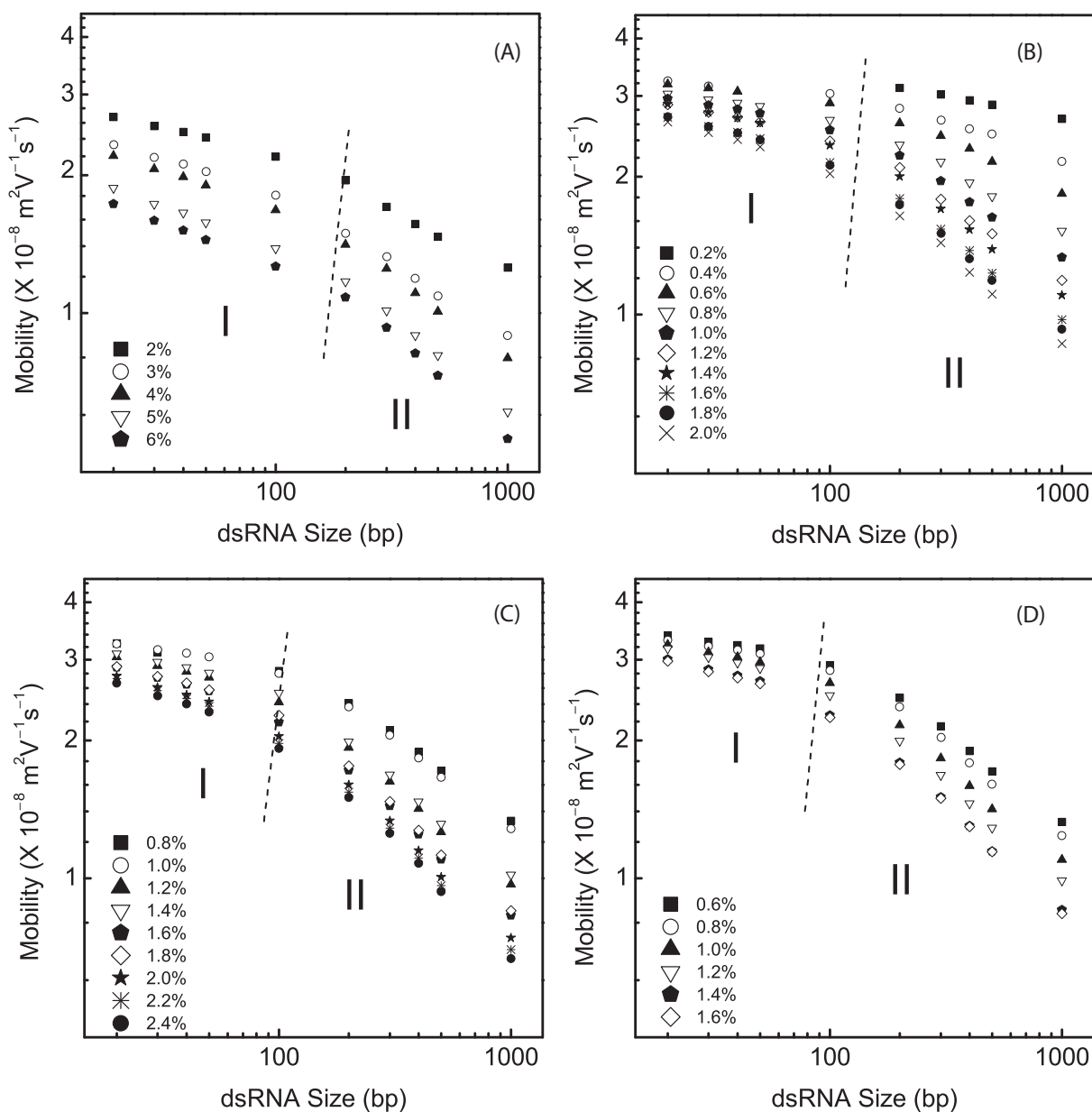


**Figure 2.** The double logarithmic plot of the mobility versus dsRNA fragment size in HEC solution with  $M_w$  of (A) 90 k, (B) 250 k, (C) 720 k, and (D) 1300 k. CE conditions were the same as Fig. 1.

experiment, 720 and 1300 k HEC solutions resolved smaller  $RL$  for 20–1000 bp dsRNA than 90 and 250 k HEC solutions.

We found that both the concentration and the  $M_w$  of HEC solution had an influence on the  $RL$  of dsRNA fragments. Small  $RL$  was obtained when the concentration increased. Besides, (1) in 90 and 250 k HEC solutions (Fig. 3A and B), the  $RL$  derived from large dsRNA fragments (200–1000 bp) was significantly influenced by HEC concentration, while the influence of HEC concentration on  $RL$  derived from small dsRNA fragments (20–100 bp) was not obvious. For example, when the concentration of 90 k HEC increased from 2 to 6%, the value of  $RL$  derived from 400 to 500 bp dsRNA decreased by 22.2 bp. And the values of  $RL$  derived from 20 to 30 bp dsRNA were only 1.1 bp difference. (2) When the

concentration of 720 k HEC increased, the  $RL$  decreased without showing size dependence on dsRNA fragments (Fig. 3C). (3) In 1300 k HEC solutions, the influence of HEC concentration on  $RL$  was significant among small dsRNA fragments, while the influence on  $RL$  was less obvious among large dsRNA fragments (Fig. 3D).

### 3.3 Size analyzing of GAPDH siRNA by CE in HEC solution

In practice, we examined GAPDH siRNA fragment for size analysis by CE. GAPDH siRNA has been used as a positive control for RNAi research [40]. We mixed the GAPDH siRNA

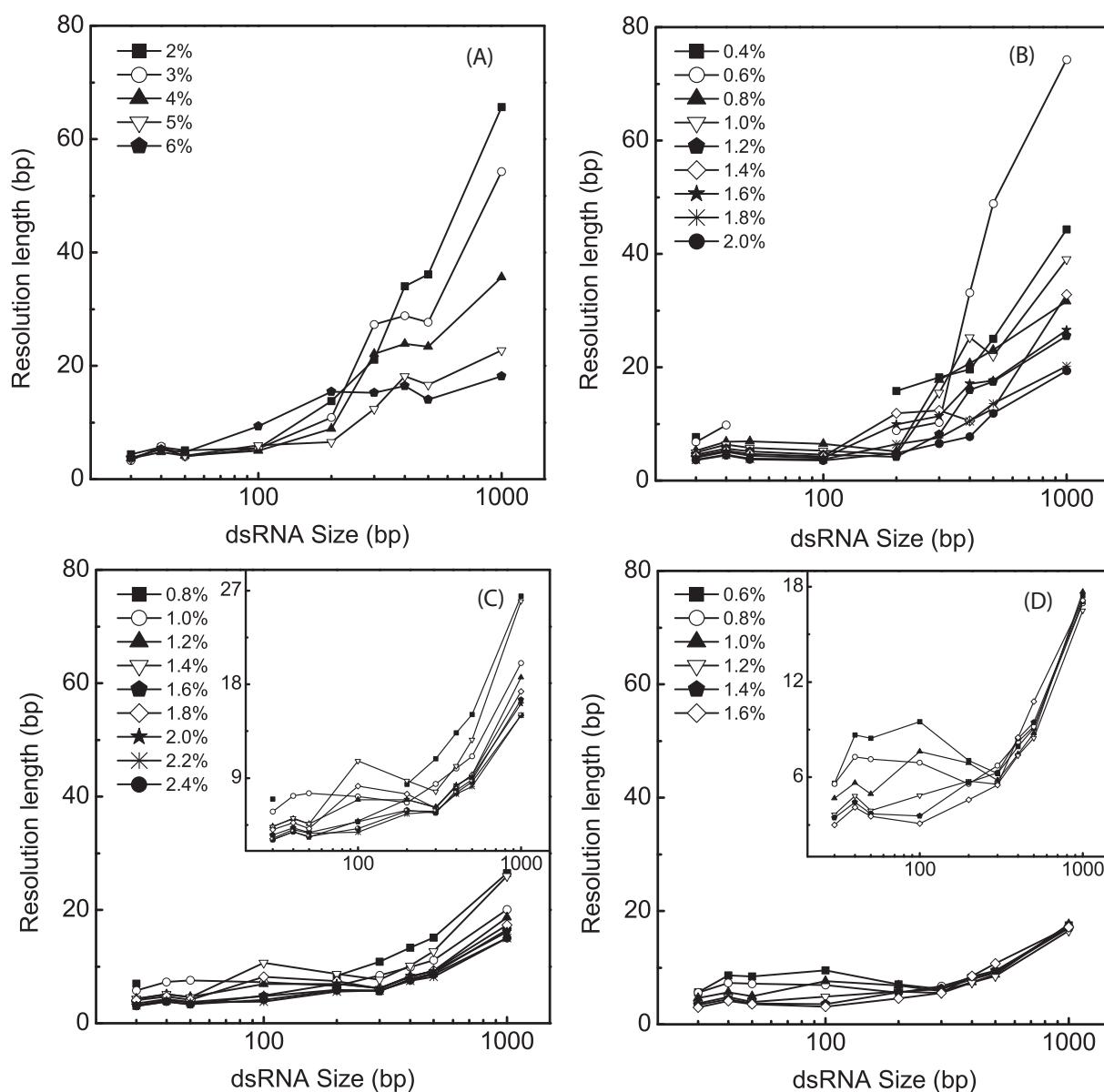


**Figure 3.** The plot of *RL* versus logarithmic dsRNA fragment size in HEC solution with *M<sub>w</sub>* of (a) 90 k, (b) 250 k, (c) 720 k, and (d) 1300 k. *RL* of one dsRNA fragments referred to the *RL* between this dsRNA fragment and the previous dsRNA fragment. CE conditions were the same as Fig. 1.

with siRNA ladder marker and then separated this mixture by our CE system. In Fig. 4A, the GAPDH siRNA fragment appeared between 20 and 30 bp dsRNA fragments at 3.6 min. For size determination, we made a plot of dsRNA fragment size (*n*) (20–400 bp) and their migration time (*t*) and found a liner relationship between them. Polynomial fitting was proceeded among raw data derived from Fig. 4A. The equation of the fitted curve was as follows:

$$t = 0.0106n + 3.3805. \quad (1)$$

And the multiple correlation coefficient ( $R^2$ ) was 0.9986. According to the liner relationship, the fragment size of

GAPDH siRNA was calculated as 20.9 bp based on its migration time. The equation was from our CE experiment.

## 4 Concluding remarks

The separation of dsRNA by CE was performed in HEC polymer solutions with various combinations of *M<sub>w</sub>* and concentration. We found two migration regimes of dsRNA in CE from the mobility plots, which were corresponded to Ogston regime and reptation without orientation. The analysis of *RL* of dsRNA fragments showed that both the concentration and the *M<sub>w</sub>* of HEC had an influence on the *RL* of dsRNA



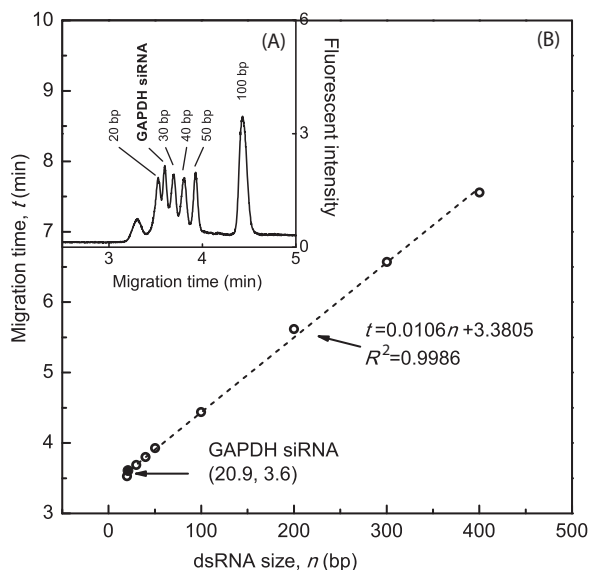


**Figure 4.** (A) Capillary electropherogram of GAPDH siRNA separation by CE in 1.2% HEC (1300 k) solution. (B) Size analysis of GAPDH siRNA, linear fitting was proceeded based on the data derived from (A). CE conditions were the same as Fig. 1.

fragments. Furthermore,  $RL$  derived from small dsRNA was more influenced by high  $M_w$  of HEC, and  $RL$  derived from large dsRNA fragments was more influenced by low  $M_w$  of HEC. The electrophoretic comparison of dsRNA and dsDNA during CE demonstrated that structural conformation between them differentiated the migration behavior. At the end, we applied CE for the separation of GAPDH siRNA. This work represents analysis of dsRNA by CE in HEC solutions, and demonstrates that CE is an efficient method for siRNA identification.

This project was partly supported by *Grand-in-Aid for Scientific Research (Houga)* (no. 25600049 [Y. Y.]), JSPS, Japan and *The Innovation Fund Project for Graduate Student of Shanghai* (no. JWCXSL1401), China.

The authors have declared no financial/commercial conflict of interest.

## 5 References

- [1] Fire, A. X., Si, Q., Montgomery, M. K., Kostas, S. A., Driver, S. E., Mello, C. C., *Nature* 1998, 391, 806–811.
- [2] Hamilton, A. J., Baulcombe, D. C., *Science* 1999, 286, 950–952.
- [3] Elbashir, S. M., Harborth, J., Lendeckel, W., Yalcin, A., Weber, K., Tuschl, T., *Nature* 2001, 411, 494–498.
- [4] Seiffert, S., Debelak, H., Hadwiger, P., Jahn-Hofmann, K., Roehl, I., Vornlocher, H.-P., Noll, B., *Anal. Biochem.* 2011, 414, 47–57.
- [5] Schmitz, J. C., Chen, T. M., Chu, E., *Cancer Res.* 2004, 64, 1431–1435.
- [6] Agrawal, N., Dasaradhi, P. V., Mohammed, A., Malhotra, P., Bhatnagar, R. K., Mukherjee, S. K., *Microbiol. Mol. Biol. Rev.* 2003, 67, 657–685.
- [7] Stellwagen, N. C., Stellwagen, E., *J. Chromatogr. A* 2009, 1216, 1917–1929.
- [8] Anderson, G. J. C., Cynthia, M., Kennedy, Robert, T., *Anal. Chem.* 2011, 83, 1350–1355.
- [9] Bannore, Y. C., Chenault, K. D., Melouk, H. A., Rassi, Z. E., *J. Sep. Sci.* 2008, 31, 2667–2676.
- [10] Fukushima, Y., Naito, T., Sueyoshi, K., Kubo, T., Kitagawa, F., Otsuka, K., *Anal. Chem.* 2014, 86, 5977–5982.
- [11] Rauch, J. N., Nie, J., Buchholz, T. J., Gestwicki, J. E., Kennedy, R. T., *Anal. Chem.* 2013, 85, 9824–9831.
- [12] Shimura, K., Kasai, K., *Electrophoresis* 2014, 35, 840–845.
- [13] Karenga, S., Rassi, Z. E., *Electrophoresis* 2011, 32, 1044–1053.
- [14] Guttman, A., *Nature* 1996, 380, 461–462.
- [15] Karger, B. L., *Nature* 1989, 339, 641–642.
- [16] Zhang, X., McGown, L. B., *Electrophoresis* 2013, 34, 1778–1786.
- [17] Kitagawa, F., Otsuka, K., *J. Chromatogr. A* 2014, 1335, 43–60.
- [18] Hüge, B. J., Flaherty, R. J., Dada, O. O., Dovichi, N. J., *Talanta* 2014, 130, 288–293.
- [19] Brinet, D., Kaffy, J., Oukacine, F., Glumm, S., Ongeri, S., Taverna, M., *Electrophoresis* 2014, 35, 3302–3309.
- [20] Viovy, J. L., *Rev. Mod. Phys.* 2000, 72, 813–872.
- [21] Slater, G. W., Kenward, M., McCormick, L. C., Gauthier, M. G., *Curr. Opin. Biotechnol.* 2003, 14, 58–64.
- [22] Barron, A., Sunada, W., Blanch, H., *Electrophoresis* 1996, 17, 744–757.
- [23] Vakonakis, I., LiWang, A. C., *J. Am. Chem. Soc.* 2004, 126, 5688–5689.
- [24] Nakano, S., Kanzaki, T., Sugimoto, N., *J. Am. Chem. Soc.* 2004, 126, 1088–1095.
- [25] Todorov, T. I., Morris, M. D., *Electrophoresis* 2002, 23, 1033–1044.
- [26] Barron, A., Soane, D., Blanch, H., *J. Chromatogr. A* 1993, 652, 3–16.
- [27] Yamaguchi, Y., Todorov, T. I., Morris, M. D., Larson, R. G., *Electrophoresis* 2004, 25, 999–1006.
- [28] Liu, C., Li, Z., Meng, F., Ni, Y., Dou, X., Yamaguchi, Y., *Acta Chim. Sinica* 2013, 71, 265–270.
- [29] Li, Z., Liu, C., Yamaguchi, Y., Ni, Y., You, Q., Dou, X., *Anal. Methods* 2014, 6, 2473–2477.
- [30] Li, Z., Liu, C., Dou, X., Ni, Y., Wang, J., Yamaguchi, Y., *J. Chromatogr. A* 2014, 1331, 100–107.
- [31] Li, Z., Chen, S., Liu, C., Zhang, D., Dou, X., Yamaguchi, Y., *J. Chromatogr. A*, 2014, 1361, 286–290.
- [32] Hjertén, S., *J. Chromatogr. A* 1985, 347, 191–198.
- [33] Slater, G., Guillouzie, S., Gauthier, M., Mercier, J., Kenward, M., McCormick, L., Tessier, F., *Electrophoresis* 2002, 23, 3791–3816.

- [34] Albarghouthi, M. N., Barron, A. E., *Electrophoresis* 2000, 21, 4096–4111.
- [35] Heller, C., *Electrophoresis* 2001, 22, 629–643.
- [36] Ogston, A. G., *Trans. Faraday Soc.* 1958, 54, 1754–1757.
- [37] de Carmejane, O., Yamaguchi, Y., Todorov, T. I., Morris, M. D., *Electrophoresis* 2001, 22, 2433–2441.
- [38] Todorov, T. I., de Carmejane, O., Walter, N. G., Morris, M. D., *Electrophoresis* 2001, 22, 2442–2447.
- [39] Slater, G. W., Desruisseaux, C., Hubert, S. J., *Methods Mol. Biol.* 2001, 162, 27–42.
- [40] Meng, Z., Zhang, X., Wu, J., Pei, R., Xu, Y., Yang, D., Roggendorf, M., Lu, M., *PLoS One* 2013, 8, e64708.